Experimental Analysis of Waveguide-coupled Surface-plasmon-polariton Cone Properties

Charles K. A. Nyamekye,[†, ‡] Qiaochu Zhu,[‡] Russell Mahmood,[ξ] Stephen C. Weibel, [δ] Andrew C. Hillier[†, ξ] and Emily A. Smith[*, †, ‡]

[†] U.S. Department of Energy, The Ames Laboratory, Ames, Iowa 50011, United States
[‡] Department of Chemistry, Iowa State University, Ames, Iowa 50011, United States
[ξ] Department of Chemical and Biological Engineering, Iowa State University, Ames, Iowa 50011, United States
[δ] Surface Photonics Inc., Madison, Wisconsin 53719, United States
[*] Corresponding Author (esmith1@iastate.edu, 1-515-294-1424)

ORCID ID
Charles K. A. Nyamekye: 0000-0002-5190-3213
Qiaochu Zhu: 0000-0002-1187-1608
Russell Mahmood: 0000-0001-9295-030X
Stephen C. Weibel: 0000-0002-5910-9671
Andrew C. Hillier: 0000-0002-2729-1368
Emily A. Smith: 0000-0001-7438-7808

Abstract

Experimental data for waveguide-coupled surface-plasmon-polariton (SPP) cones generated from dielectric waveguides is presented. The results demonstrate a simpler route to collect plasmon waveguide resonance (i.e., PWR) data. In the reverse-Kretschmann configuration (illumination from the sample side) and Kretschmann configuration (illumination from the prism side), all the waveguide modes are excited simultaneously with p- or s-polarized incident light, which permits rapid acquisition of PWR data without the need to scan the incident angle or wavelength. The concentric SPP cone properties depend on the thickness and index of refraction of the waveguide. The angular intensity pattern of the cone is well-matched to simulation results in the reverse-Kretschmann configuration, and is found to be dependent on the polarization of the incident light and the polarization of the waveguide mode. In the Kretschmann geometry, all waveguide-coupled SPP cones are measured at incident angles that produce attenuated light reflectivity. In addition, the enhanced electric field produced under total internal reflection allows high signal-to-noise ratio multimodal spectroscopies (e.g., Raman scattering, luminescence) to measure the chemical content of the waveguide film, which traditionally is not measured with PWR.

Introduction

Surface-plasmon-polariton-coupled analysis techniques are useful methods for studying thin films, optical waveguides, and for monitoring real-time adsorption of molecules onto a metal surface.[1-11] Plasmon waveguide resonance (PWR), for example, uses both p- and s-polarized incident light to generate guided modes within a waveguide dielectric material.[12-14] In a typical PWR experiment, the reflectivity of light is monitored from a prism/waveguide film as a function of incident angle or wavelength. PWR is particularly useful for measuring the properties of anisotropic films.

Two common illumination geometries used in SPP-coupled spectroscopies are the Kretschmann (Figure 1) and reverse-Kretschmann (Figure 2) configurations. Both configurations consist of an optically-coupled lower-refractive-index sample, a thin metal film and a higher-refractive-index prism. When surface plasmons are excited in the Kretschmann configuration, a hollow cone of directionally scattered light (the surface-plasmon-polariton cone, or SPP cone) is generated on the prism side at a defined angle due to momentum conserving optical and roughness coupling.[15] The collection of the SPP cone from a prism/55-nm silver film/air interface onto photographic film was demonstrated by Simon and Guha in 1976.[16] We recently reported an optical setup for collecting the full SPP cone image as a function of incident angle as well as the quantification of the SPP cone properties for a thiophenol monolayer and thin (< 100-nm) polymer films.[1]

A SPP cone can also be produced in the reverse-Kretschmann configuration, wherein the incident laser illuminates from the sample side with an orientation that is perpendicular to the interface. The angular intensity of the SPP cone (defined in Figure 3) on the prism side varies with both the polarization of the incident light and the scattered light. Braundmeier and

Tomaschke[15] reported on the angular intensity patterns of the SPP cone with p- and s-polarized light incident on the air/Ag/prism interface in the reverse-Kretschmann configuration. A single SPP cone with a nonuniform angular intensity pattern was observed. The maximum cone intensity was recorded in the vertical plane for s-polarized incident light and horizontal plane for p-polarized light. The authors concluded that the maximum intensities around the SPP cone match the orientation of the incoming photons, although the angular intensity pattern of the SPP cone was not modeled.

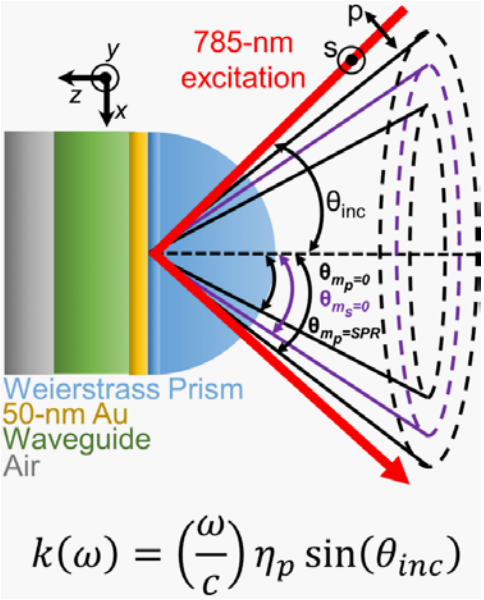

Figure 1. Schematic of the Kretschmann configuration., Multiple concentric SPP cones are measured for the analysis of waveguide samples. A Weierstrass prism is a hyper-hemisphere, which enables the full SPP cone to be measured. Surface plasmons are excited when the wave vector $k(\omega)$ of incident light with frequency ω and incident angle θ_{inc} traveling through a prism with index of refraction η_p matches the electron oscillation frequency of the metal substrate, where c is the speed of light in a vacuum.

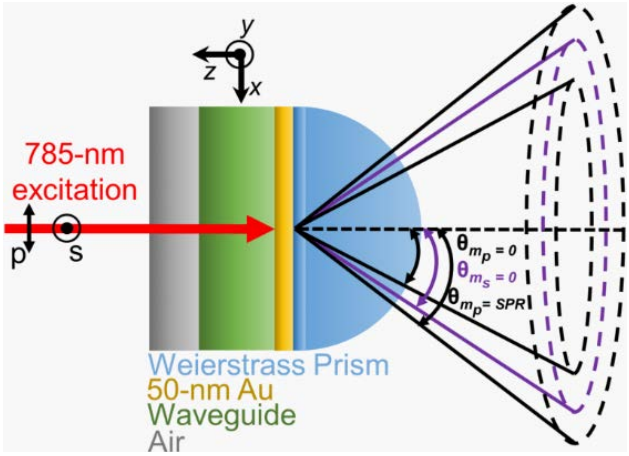

Figure 2. Schematic of the reverse-Kretschmann configuration. Illumination is from the sample side and the incoming rays are at normal incidence to the sample.

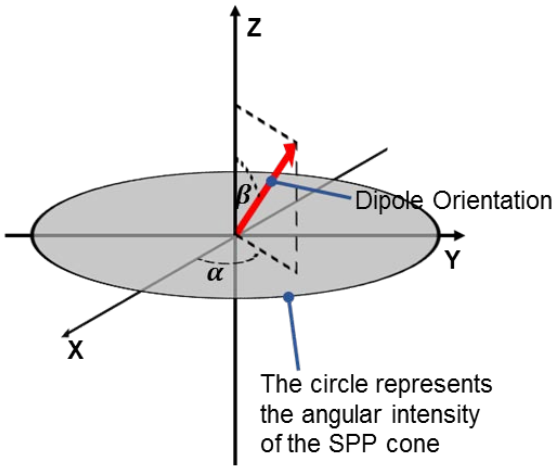

Figure 3. The angular intensity of the SPP cone is the intensity of light as α is rotated from 0° to 360°. The parameter β describes the orientation of the dipole producing the signal.

Previous reports showing SPP cones did not study waveguide films, rather they focused on bare metal films or thin films that did not meet the waveguide criterion. Plasmon waveguide structures consist of a thin metal film coated with a dielectric layer of thickness ~ $\frac{\lambda}{2\eta}$ or greater,

where λ is the excitation wavelength and η is the dielectric material's refractive index.[17, 18] Several waveguide-coupled spectroscopies have been reported that enable sensitive measurements as a result of the enhanced signals produced by the resonant excitation of electromagnetic modes in the waveguide structure.[14, 19-21] To date, these techniques have not relied on measurements of the waveguide-coupled SPP cones, despite the useful information that they encode and the simplicity of not needing to scan the incident angle or wavelength of light. This may be in part due to the lack of experimental data for waveguide-coupled SPP cones. (Experimental measurements have been projected onto tracing paper and photographed for surface-plasmon-coupled emission (SPCE) originating from fluorophores located in close proximately to a metallic surface.[22-26])

Simulations of SPCE and waveguide-coupled SPP cones have been reported by Nils Calander[27] and Zhi-Mei Qi,[28, 29] respectively. Calander's simulation was based on Fresnel's equations and the Weyl identity theorem for expressing the electromagnetic energy density of the SPCE from a dipole inside a thin polymer film. The simulation results were comparable to the experimental SPCE results of Gryczynski, Lakowicz, and Malicka.[22, 24, 30, 31] Qi and coworkers' simulations were based on Fresnel's equations and optical reciprocity theorem.[28, 29] They simulated a plasmon waveguide structure in the Kretschmann configuration with a dipole emitter positioned at various locations within the waveguide dielectric layer, which was placed between a gold film and an air layer. The authors concluded that the angular intensity of the waveguide-coupled SPP cones was greatly influenced by the dipole's orientation and distance from the metal surface. No experimental waveguide-coupled SPP cone data were presented.

Herein, we report the experimentally measured properties of waveguide-coupled SPP cones with reverse-Kretschmann and Kretschmann illumination geometries. The experimental

properties measured in the reverse-Kretschmann configuration include the angular intensity patterns of the waveguide-coupled SPP cones, their polarization dependence, and cone angles. In the Kretschmann configuration, in addition to images of the waveguide-coupled SPP cones, the directional Raman signal is also recorded. The signals are well modeled using standard optical modeling[27, 32] and three-dimensional finite-difference time-domain simulations. We propose that the waveguide-coupled SPP cone properties reported herein enable a simple and information-rich method for collecting plasmon waveguide resonance data in a single image without the need to scan the incident angle or frequency of light during data collection.

Experimental Method

Sample preparation

The waveguide samples were prepared on 25.4 mm diameter sapphire substrates obtained from Meller Optics (Providence, RI). Prior to preparing the waveguide films, a 2-nm titanium (99.999% pure Ti) adhesive layer and 50-nm gold (99.999% pure Au) layer were deposited on clean sapphire disks. The metal deposition was performed by Platypus Technologies LLC., Madison, WI. The gold films were immersed in piranha solution (3:1 mixture of sulfuric acid (assay 99.999%, CAS# 7664-93-9, Sigma-Aldrich St. Louis, MO) and hydrogen peroxide (assay 31.7%, CAS# 7722-84-1, Fisher Chemical Pittsburgh, PA) for three minutes to ensure a clean gold surface. **[Piranha solution will cause chemical and thermal burns if not handled with extreme caution]**. Deionized water from an 18.2 MΩ cm^{-1} EasyPure II filtration system (Thermo Scientific, Waltham, MA) was used to rinse the gold films after the piranha cleaning process. A 50:50 (v/v) 200 proof ethanol (assay 99.5%, CAS# 64-17-5, Sigma-Aldrich St. Louis,

MO) and deionized water mixture was prepared for sonicating the gold films for 5 minutes with an ultrasonic cleaner followed by drying in a stream of N_2 gas.

A sputter-up-type sputtering system (ATC 1800-F, AJA International, Scituate, MA) was used for RF sputtering ~400-nm of silica (SiO_2, purity 99.0-99.9999%) onto a 2-nm Ti/50-nm Au coated sapphire disk substrate. The sputtering system was equipped with a quartz crystal thickness monitor (TM-350/400, Maxtek Inc, Cypress, CA). Silica sputtering was achieved using a RF power of 135 W, argon pressure of ~3 mTorr and a substrate rotation rate of 20 rpm. Poly(methyl methacrylate) (PMMA, M_w = ~120,000, CAS# 9011-14-7) and polystyrene (PS, M_W = 192,000, CAS# 9003-53-6) were purchased from Sigma-Aldrich (St. Louis, MO) and prepared in anhydrous toluene (assay 99.8%, CAS# 108-88-3, Fisher Chemical Pittsburgh, PA) at concentrations of 0.10005 and 0.1030 g ml^{-1} of PMMA and 0.0255, 0.0785, 0.0814, and 0.0926 g ml^{-1} of PS. Poly(4-vinylphenol) (PVPh, M_w = ~11,000, CAS# 24979-70-2) purchased from Sigma-Aldrich (St. Louis, MO) was prepared in 200 proof ethanol at concentrations of 0.08997 and 0.1119 g ml^{-1}. All the waveguide films were then prepared by spin coating 200 µL of the PMMA, PS, and PVPh solutions on separate gold-coated sapphire disks at 3000 rpm for one minute using a KW-4A spin coater (Chemat Technology, Inc. Northbridge, CA). A 0.0255 g ml^{-1} PS solution was spin-coated on top of ~400 nm silica waveguide film after data were collected for the bare silica film. The polymer waveguides were left to dry overnight in ambient conditions to make certain the solvent was completely evaporated.

The thickness of nine waveguide films was measured using a spectroscopic ellipsometer (J. A. Woollam α-SE, J. A. Woollam Co. Inc., Lincoln, NE, USA) operating in the wavelength range of 380-900 nm at 65°, 70° and 75° angles of incidence with a 10 second data acquisition rate. The measured psi (Ψ) and delta (Δ) parameters were fit to multilayer film models using the

CompleteEase™ software package. The refractive index η and absorption coefficient *k* of the gold substrate were first determined using a two-phase air/gold substrate model. The thicknesses of the silica and polymer films were then determined by fitting ellipsometry data to three- and four-layer air/waveguide/gold substrate models. Measurements were taken at five different locations on the samples and an average thickness and standard deviation of the waveguide films were computed (Table 1). Subsequently, the refractive index of a bulk poly(4-vinylphenol) film was determined at 785 nm (i.e., the excitation wavelength of the near-infrared laser used to collect the experimental data) by ellipsometry.

TABLE 1. Thicknesses of the indicated waveguide dielectric samples.

concentration (g mL^{-1})	**ellipsometry thickness (nm)[2]**
SiO_2	354 ± 1
0.0255 PS : SiO_2 [1]	454 ± 10
0.0900 PVPh	404 ± 2
0.1001 PMMA	411 ± 5
0.1119 PVPh	496 ± 3
0.1030 PMMA	516 ± 3
0.0785 PS	543 ± 1
0.0814 PS	602 ± 8
0.0926 PS	717 ± 2

1 The waveguide sample consists of PS on top of a SiO_2 waveguide substrate (SiO_2 : PS).
2 The uncertainties represent the standard deviations from five different locations on the sample.

Waveguide-coupled SPP cone measurements

In the Kretschmann configuration (Figure 1), the gold film was coated on a sapphire substrate and optically coupled to a sapphire Weierstrass-type prism (ISP Optics Irvington, NY) with a η = 1.7400 (at the sodium D line) index matching fluid solution (Cargille Laboratories Inc., Cedar Grove, NJ). The sample holder designed to secure the prism and the gold substrate was placed on a previously described instrument.[1] In the reverse-Kretschmann configuration

(Figure 2), the laser was directed perpendicular to the sample from the front side. A digital image of the entire SPP cone was acquired with a 75 mm (*f*/1.3) Kameratori TV Lens (Tampere, Finland) attached to a 11.340 mm × 7.130 mm, 2.32 mega pixel CMOS sensor (IDS Imaging Development Systems GmbH, Obersulm, Germany).[1] The SPP cone was acquired with both p- and s-polarized illumination. A near-infrared polarizer was used to further enhance the linearly polarized laser and a half-waveplate was used to switch between p- and s-polarized light. Translational mirrors were controlled by software integrated with a stepper motor used to scan the incident angle from 0.00° to 65.00° with 0.06° angle resolution. The experimental waveguide-coupled SPP cone diameter was determined from a CMOS calibration image of a ruler placed between the Weierstrass prism and the collection lens (Figure S1).

Waveguide-coupled directional Raman measurements

In the Kretschmann configuration, directional Raman scattering was measured as a function of incident angle with p- and s-polarized 200 mW 785-nm light. The spectra were acquired with either 30 or 60 s acquisitions for 3 accumulations at the angle that produced the most intense SPP cone intensity. Three replicate measurements were obtained for each sample. All spectra were collected at room temperature.

Simulation of the electric field intensity distribution around the waveguide-coupled directional-surface-plasmon-polariton cones

Data were modeled using standard optical calculations.[27, 32] Three-dimensional finite-difference-time-domain (FDTD) simulations (EM Explorer, San Francisco, CA) were used to calculate the angular intensity pattern around the cone by looping over alpha (α) while

computing the scattered field in planes orientated in different radial directions (Figure 3). The angle α was scanned between 0° to 360° with 3° resolution at an excitation wavelength of 785 nm. The base interface included a sapphire prism (η 1.7619), gold film (η 0.1431 + 4.799*i*), waveguide, and air (η 1.000). The thicknesses of the prism and air layers were semi-infinite compared to the waveguide (≥ 300 nm) and the gold (50 nm) layers. The dielectric waveguide materials were: silica (η 1.454), poly(methyl methacrylate) (η 1.48452), polystyrene (η 1.57826), or poly(4-vinylphenol) (η 1.560) of varying thicknesses (Table 1). The calculations assumed all layers were homogenous. A scattering dipole was placed at the center of the waveguide layer between the gold and air layers (Figure S2). The orientation of the scattering dipole was given by the beta (β) parameter (Figure 3). The *calculated* waveguide-coupled SPP cone diameter was determined using the SPP cone angle obtained from the simulations and the inverse-tangent of the distance between the prism (i.e., sample interface) and detector. A Python (v3.6) script with Matplotlib plotting library was implemented to plot a 2D representation of the log of the angular electric field intensity around the concentric cones as a function of cone angle.

Results and Discussion

Quantification and modeling of the waveguide-coupled SPP cones with reverse-Kretschmann Raman illumination

The experimentally measured and calculated waveguide-coupled SPP cones for a 354 ± 1 nm silica over 50-nm Au film are shown in Figure 4A. Three concentric SPP cones are observed. The spacing between the cones when comparing the experimental and calculated data do not always match. This discrepancy is the result of the optics used to image the cones, which can cause image compression, particularly at large cone angles. The image compression is

compensated for as described in Fig. S1, and the angle at which each SPP cone is generated is determined. The experimentally measured cone angle is matched with the calculated angles to assign a mode to each cone (Table 2). The inner cone corresponds to waveguide mode 0 for p-polarized light ($m_p = 0$), the middle cone corresponds to waveguide mode 0 for s-polarized light ($m_s = 0$), and the outer cone corresponds to the SPR mode. As expected, the SPP cone image is rotated by 90° when the incident light is switched from p to s polarization (Figure 4A). Figure 4B illustrates the relationship between the polarization of the incident light, the polarization of the waveguide mode, and the resulting angular intensity pattern of the SPP cone. When the polarization of the waveguide mode matches the polarization of the excitation source, the areas of maximum SPP cone intensity are in the horizontal plane using this experimental setup. In contrast, when the polarization of the waveguide modes is orthogonal to the polarization of the excitation source, the maximum cone intensity is measured in the vertical plane.

TABLE 2. Measured and calculated waveguide-coupled SPP cone angles (θ_{cone}) with illumination in the reverse-Kretschmann configuration.

ellipsometry thickness (nm)	$m_{Polarization}$ [1]	experimental θ_{cone} (°) [2]	calculated θ_{cone} (°)
354 ± 1 SiO_2	$m_p = 0$	32.15 ± 0.04	32.15
	$m_s = 0$	39.7 ± 0.2	39.90
	$m_p = SPR$	45.7 ± 0.2	45.80
454 ± 10 SiO_2 : PS	$m_p = 0$	35.36 ± 0.07	35.39
	$m_s = 0$	41.74 ± 0.02	41.72
	$m_p = SPR$	49.01 ± 0.03	49.04

1 $m_{polarization}$ = waveguide mode assignment, where the polarization is either p or s polarized; *SPR* = surface plasmon resonance

2 The uncertainties represent the standard deviation of the cone angles from the SPP cone images acquired with p- and s-polarized light

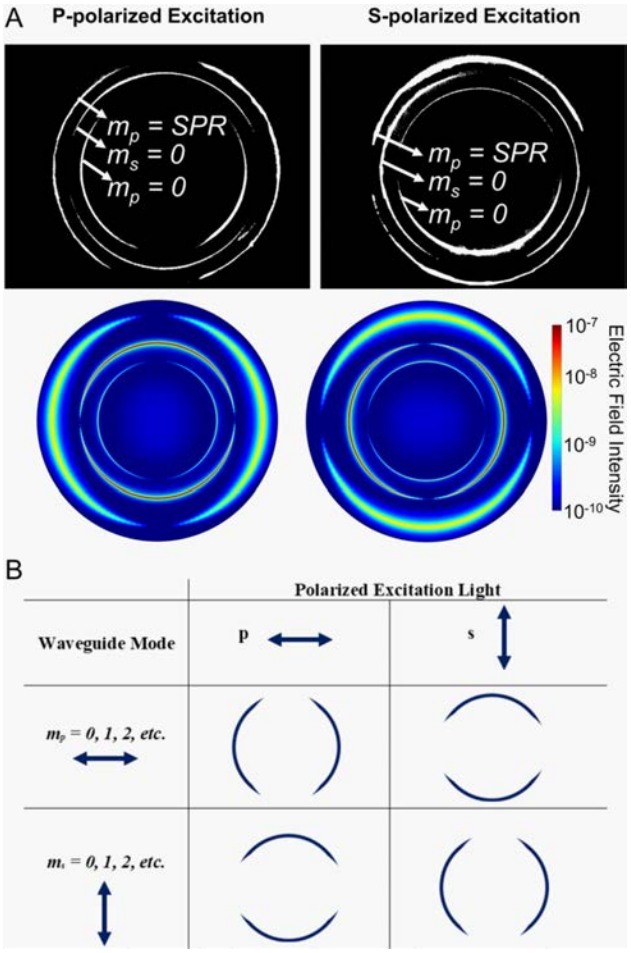

Figure 4. Experimentally measured (black/white scale) and calculated (color scale, shown in a logarithmic base 10 scale) waveguide-coupled SPP cones for a 354 ± 1 nm SiO_2 waveguide sample acquired in the reverse-Kretschmann configuration with (left) p- and (right) s-polarized incident light. The cone angles for the three waveguide modes are listed in Table 2. (B) Schematic showing the relationship between the waveguide mode assignment, the polarization of the excitation source, and the resulting angular intensity pattern in the reverse-Kretschmann configuration.

After coating a 100 ± 10 nm polystyrene film onto the 354 ± 1 nm silica waveguide substrate (SiO_2 : PS), we still observe two waveguide modes ($m_p = 0$, $m_s = 0$) and one SPR mode ($m_p = SPR$). However, all the modes appear at larger cone angles compared to the bare

silica waveguide (Figure S3 and Table 2). The waveguide-coupled SPP cone properties in the reverse-Kretschmann configuration were further tested using seven polymer waveguides with thicknesses ranging from ~400 to 720 nm. Three different polymers used to make the waveguides, including: polystyrene (index of refraction at 785 nm, $\eta = 1.57826$), poly(4-vinylphenol) ($\eta = 1.560$), and poly(methyl methacrylate) ($\eta = 1.48452$). Images of the SPP cones using p-polarized incident light are shown in Figure 5 and using s-polarized incident light in Figure S4. In this instrumental configuration, the setup allows cone angles in the range of ~30° to ~50° to be measured. SPP cones outside this range (i.e., the SPR modes for the 411 ± 5 nm and 516 ± 3 nm poly(methyl methacrylate) waveguide samples) cannot be measured with existing instrumentation due to the limiting aperture of the collection lens. It is noteworthy to mention that the calculated waveguide-coupled SPP cone for 602 ± 8 nm polystyrene waveguide film do not show the angular intensity pattern for waveguide mode $m_p = 1$ (i.e., the innermost cone denoted by dashed line), even though it is observed experimentally. This is due to the large angle resolution of 3° used for the calculation, given that the calculated FWHM from the reflectivity plot is much less than 3°.

Both the thickness and the index of refraction of the waveguide affect the waveguide-coupled SPP cone properties. There is an increase in the number of waveguide-coupled SPP cones with increasing polymer thickness,[17] with four cones measured for the thickest 717 ± 2 nm polystyrene waveguide. Figure 6 shows the cone angles for all seven polymer waveguide films. When considering the same polymer material, the cone angle for a particular waveguide mode increases with increasing thickness (Figure 6 and Table S1). When considering the reverse-Kretschmann cone angle and the data for the polystyrene waveguides, the sensitivity of the measurement is 0.009°/nm ($m_s=0$), 0.02°/nm ($m_p=0$), 0.03°/nm ($m_s=1$) and 0.02°/nm ($m_p=1$).

Abbas *et al.* report a PWR sensitivity of 0.010°/nm using a 510-nm silica waveguide and a gold film with a scanning angle (i.e., reflectivity) measurement.[33] While not all experimental parameters are equal, this does show the sensitivity of the waveguide-coupled SPP cone measurement is similar to reported PWR experiments. Abbas *et al.* also report a higher sensitivity using a silver film, which would also be expected for the measurements of the waveguide-coupled SPP cone.

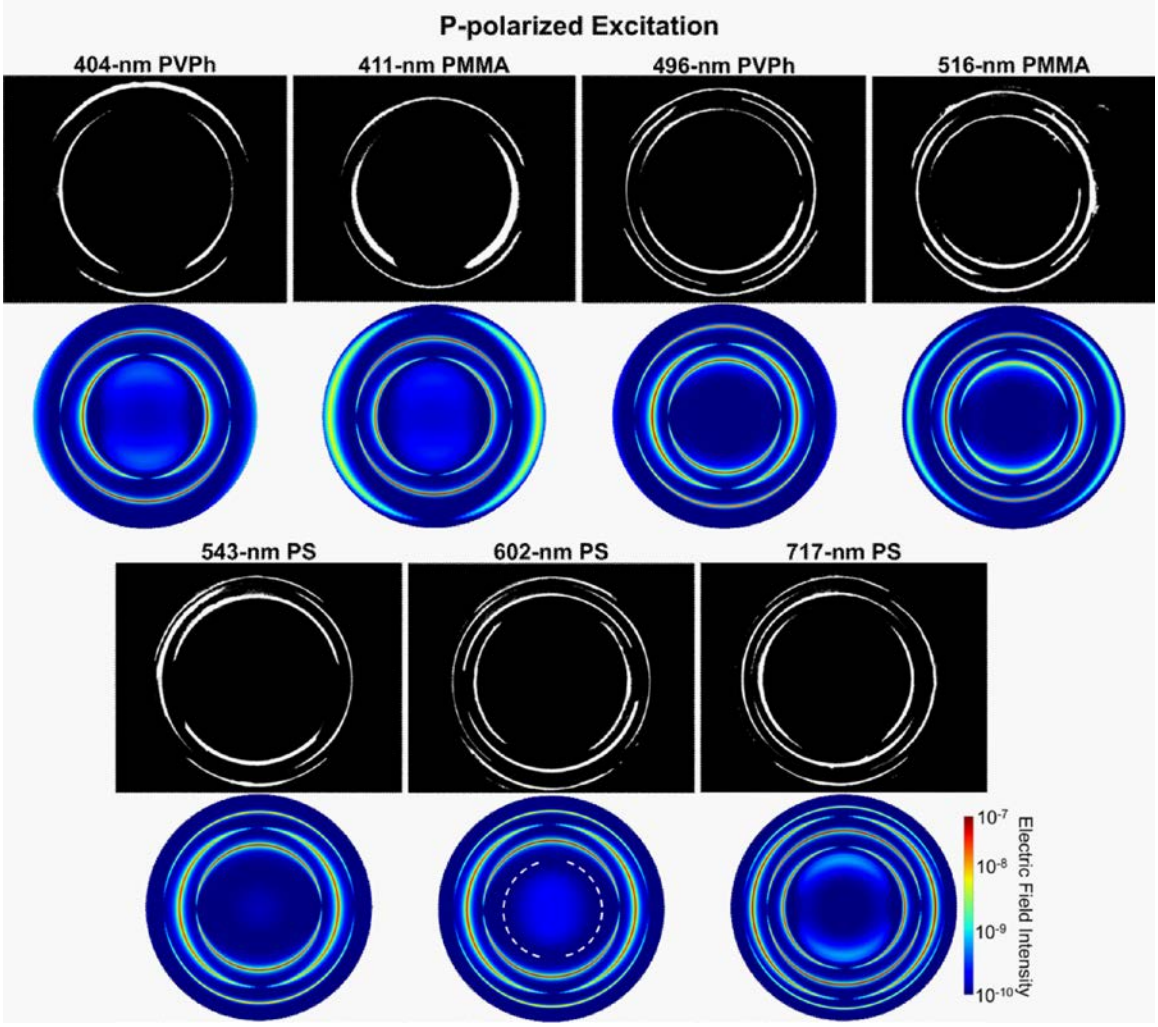

Figure 5. Experimentally measured (black/white scale) and calculated (color scale, shown in a logarithmic base 10 scale) waveguide-coupled SPP cones showing the angular intensity patterns for 404 ± 2 nm poly(4-vinylphenol) (PVPh), 411 ± 5 nm poly(methyl methacrylate) (PMMA),

496 ± 3 nm PVPh, 516 ± 3 nm PMMA, 543 ± 1 nm polystyrene (PS), 602 ± 8 nm PS and 717 ± 2 nm PS waveguide structures with reverse-Kretschmann p-polarized illumination. The experimental and calculated cone angles are listed in Table S1, and data using s-polarized incident light are shown in Figure S4. The angle resolution used for the calculation is 3°, and the inner cone for the 602 ± 8 nm polystyrene waveguide (which has a FWHM of much less than 3°) does not show in the calculation. The missing inner cone is represented by the dashed white lines in the calculated angular intensity pattern for 602 ± 8 nm PS waveguide.

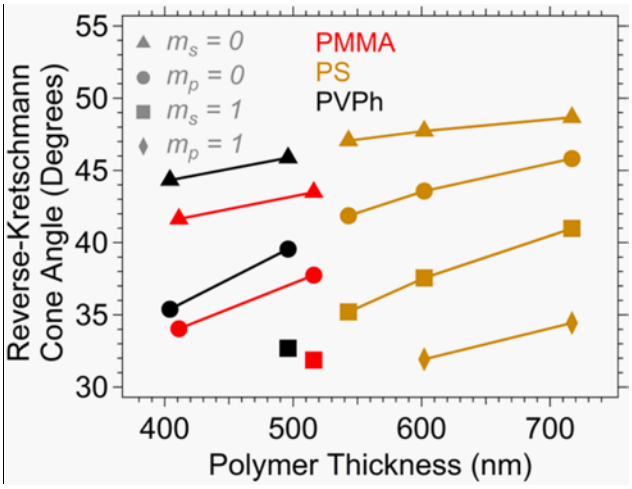

Figure 6. Plot of the reverse-Kretschmann cone angles as a function of polymer thickness for each waveguide mode represented by the symbols (▲) $m_s = 0$, (●) $m_p = 0$, (■) $m_s = 1$, and (♦) $m_p = 1$ generated from (red trace) PMMA, (gold trace) PS, and (black trace) PVPh. The experimental and calculated cone angles are listed in Table S1. The error bars representing the standard deviation of the cone angles are not visible on this scale (the average standard deviation is 0.04°).

Waveguide-coupled SPP cone angular intensity pattern and directional Raman scattering measurements with Kretschmann illumination

In the Kretschmann configuration, there are two relevant angles: the angle of incident light that produces the SPP cones (θ_{inc}) and the angle at which the SPP cones are projected (θ_{cone}). The incident angle is always larger than SPP cone angle. The incident angles at which the waveguide modes are generated correlate with the calculated attenuation of the reflected light (Figure 7). Both the incident and SPP cone angles are shifted to higher values when 100 ± 10 nm polystyrene is coated over the 354 ± 1 nm silica film, as expected. There is a wider angle range over which the SPP cones are measured compared to the calculated reflectivity, which is a result of a small angle spread in the incident angle.

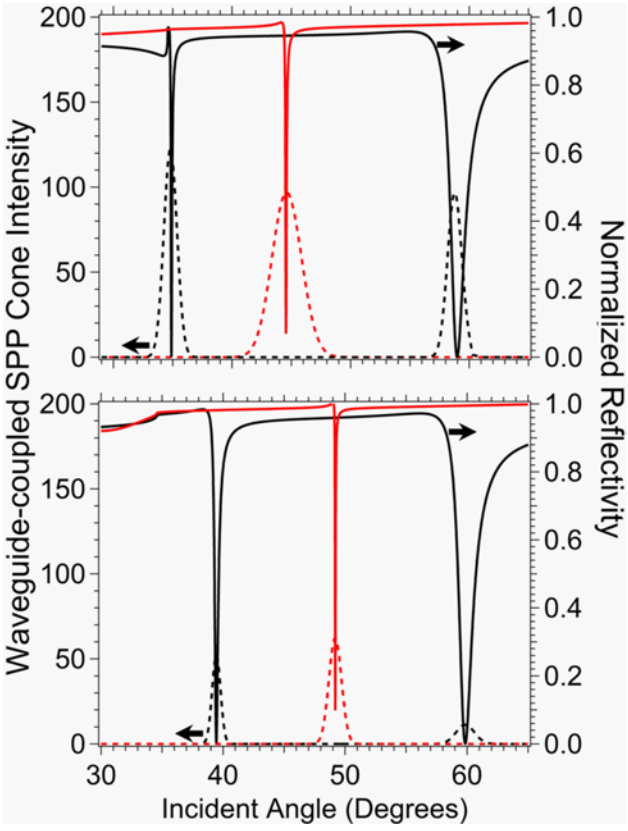

Figure 7. Experimentally measured waveguide-coupled SPP cone intensity acquired in the Kretschmann configuration (dotted line) and calculated Fresnel reflectivity (solid line) for (top) 354 ± 1 nm SiO_2 and (bottom) 354 ± 1 nm SiO_2 : 100 ± 10 nm PS waveguide films. The red and black curves correspond to s- and p-polarized incident light, respectively. The experimental/calculated incident angles (θ_{inc}) for the bare SiO_2 waveguide modes are: 34.80°/34.88° ($m_p = 0$); 44.58°/44.54° ($m_s = 0$); and 58.77°/58.98° ($m_p = SPR$). The experimental/calculated incident angles for the SiO_2 : PS waveguide modes are: 39.44°/39.42° ($m_p = 0$); 49.19°/49.19° ($m_s = 0$); and 59.79°/59.79° ($m_p = SPR$).

Images of the SPP cones were collected at every incident angle at which the reflected light intensity was maximally attenuated in the Kretschmann configuration (Table S2). The waveguide-coupled SPP cone image acquired at an incident angle of 34.80° (the incident angle associated with $m_p = 0$) for the 354 ± 1 nm silica waveguide is shown in Figure 8. As with reverse-Kretschmann illumination, multiple concentric SPP cones are observed. Since all the waveguide modes can be excited simultaneously with p- or s-polarized incident light at a single incident angle, this represents a simple new strategy for quantifying the properties of a waveguide, or adsorption to a waveguide, in the Kretschmann geometry. The presence of both scattered and reflected light from the through-prism illumination in the Kretschmann configuration (on the right and left of the image in Figure 8) make it difficult to measure the angular intensity pattern around the entire cone, particularly with the polymer waveguide samples. For this reason, the SPP cone intensities were only analyzed in the vertical direction where the background is minimized. The incident angles that produce SPP cones and the SPP cone angles have a linear dependence (Figure 9), which makes it straightforward to determine

the optimum incident angle for data collection. This reduces the acquisition time for collecting PWR data in the Kretschmann configuration since there is no need to scan an entire angle range to collect the SPP cones.

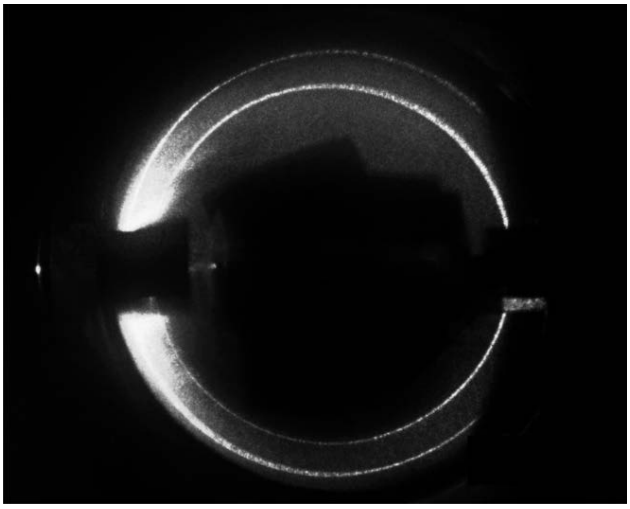

Figure 8. Waveguide-coupled SPP cone image acquired with p-polarized incident light directed at θ_{inc} = 34.80° ($m_p = 0$) in the Kretschmann configuration for the 354 ± 1 nm SiO_2 waveguide film. The inner and outer cones represent waveguide modes $m_p = 0$ and $m_s = 0$, respectively. The high background at the left of the image is from reflected and scattered light from the sapphire prism. The optics that direct the incident light (right) and block a majority of the reflected light (left) are observed in the image.

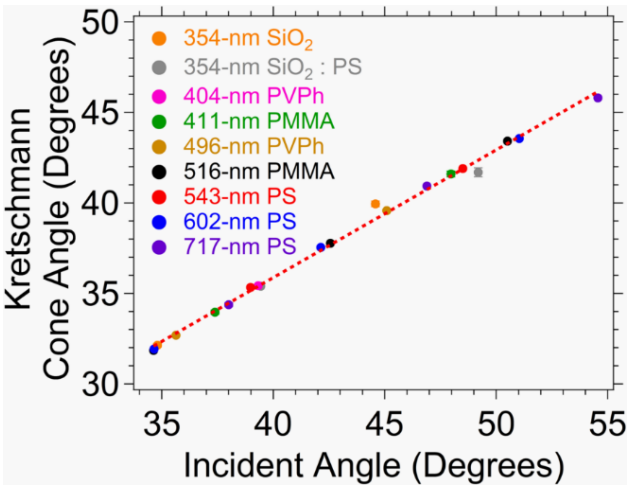

Figure 9. Experimental waveguide-coupled SPP cone angles measured in the Kretschmann configuration versus incident angle for all nine waveguide samples. The linear fit (dotted red trace) of the experimental data is [$y = 0.705x + 7.662$; $R^2 = 0.9958$]. The error bars representing the standard deviation of the SPP cone angles are not visible on this scale (the average standard deviation is 0.06°). Table S2 shows the values of the cone angles and incident angles of all nine waveguide films.

A comparison of the reverse-Kretschmann and Kretschmann cone angles is shown in Figure 10. There is a linear dependency for the cone angles acquired in both the Kretschmann-type configurations across all waveguide thicknesses, with an average deviation of 0.05° for all the data collected. This means the sensitivity (°/nm) is the same for both illumination geometries. A benefit of utilizing the Kretschmann configuration, which produces total internal reflection, is the ability to measure directional Raman signals from thin films with high signal-to-noise ratio spectra (Figure S5).[1, 7] This provides chemical information about the waveguide structure as well as the identity of the adsorbed species. None of the waveguide films produced detectable Raman

signal with the reverse-Kretschmann illumination through the air/metal/prism interface using the same instrument components.

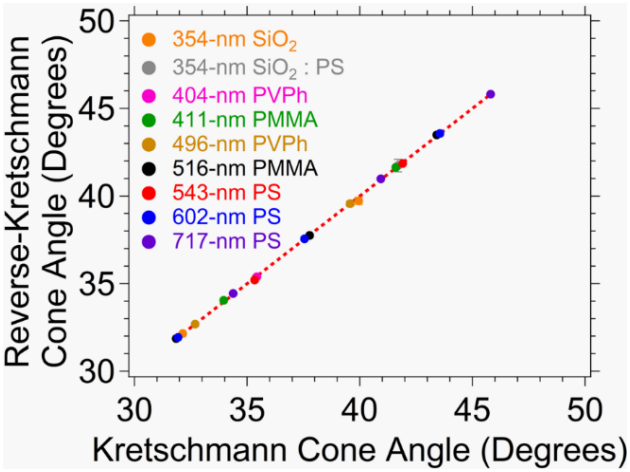

Figure 10. Plot of the experimental SPP cone angles measured in the reverse-Kretschmann configuration versus the Kretschmann SPP cone angles for all the waveguide dielectric structures. The linear fit (dotted red trace) of the experimental data is [$y = 1.001x - 0.027$; $R^2 = 0.9997$]. The error bars represent standard deviations of the SPP cone angles obtained in the two Kretschmann-type configurations and are not visible on this scale.

Conclusions

We have demonstrated method for collecting PWR data using images of SPP cones from dielectric waveguide films on a noble metal surface in both the reverse-Kretschmann and Kretschmann configurations. Waveguide properties (e.g., thickness, index of refraction) can be determined from a single SPP cone image because all the waveguide modes are excited simultaneously and observed with p- or s-polarized light. Similarly, film formation on the waveguide can also be measured. In the reverse Kretchmann geometry, there is no need for

additional optics to vary the incident angle of light, and the angular intensity pattern of the cones encodes information about polarization of the various modes. In addition, the Kretschmann configuration enables sensitive spectral measurements, such as Raman scattering for example, since the illumination conditions produce total internal reflection and enhanced electric fields at the interface. Both illumination configurations have similar sensitivities that parallel those reported in the literature for scanning angle PWR measurements, but require no moving parts to collect. Measurements of waveguide-coupled SPP cones will enable the study of morphology, composition and chemical structure for thin films, such as those found in optoelectronics, sensing devices, and in separations.

Acknowledgement

This research was supported by the U.S. Department of Energy, Office of Science, Basic Energy Sciences, Chemical Sciences, Geosciences, and Biosciences Division. The research was performed at the Ames Laboratory, which is operated for the U.S. DOE by Iowa State University under contract # DE-AC02-07CH11358.

Supporting Information (SI)

Figure S1 shows an image of the SPP cone and a metal ruler used for distance per pixel calibration. The Kretschmann-type simulation schematic used to simulate the angular intensity patterns can be found in Figure S2. Experimental and calculated waveguide-coupled SPP cones acquired in the reverse-Kretschmann configuration is shown in Figure S3 depicting the angular intensity patterns for 454 ± 10 nm SiO_2 : PS waveguide sample. Figure S4 shows the angular intensity patterns for all polymer materials (PMMA, PS, and PVPh) and thicknesses ranging from ~400 to 720 nm, with reverse-Kretschmann s-polarized illumination. Figure S5 is the

waveguide-coupled directional Raman spectra for 354 ± 1 nm SiO_2, 411 ± 5 nm PMMA, 496 ± 3 nm PVPh and 602 ± 8 nm PS on gold using p- and s-polarized light. Tables S1 summarizes the waveguide-coupled SPP cone properties for all the polymer films with reverse-Kretschmann illumination. Table S2 displays the waveguide-coupled SPP cone properties for the Kretschmann configuration.

References

1. Nyamekye, C. K. A.; Weibel, S. C.; Bobbitt, J. M.; Smith, E. A., Combined measurement of directional Raman scattering and surface-plasmon-polariton cone from adsorbates on smooth planar gold surfaces. *Analyst* **2018,** *143* (2), 400-408.

2. Futamata, M.; Borthen, P.; Thomassen, J.; Schumacher, D.; Otto, A., Application of an ATR Method in Raman Spectroscopy. *Applied Spectroscopy* **1994,** *48* (2), 252-260.

3. Futamata, M., Surface-Plasmon-Polariton-Enhanced Raman Scattering from Self-Assembled Monolayers of p-Nitrothiophenol and p-Aminothiophenol on Silver. *The Journal of Physical Chemistry* **1995,** *99* (31), 11901-11908.

4. Futamata, M.; Keim, E.; Bruckbauer, A.; Schumacher, D.; Otto, A., Enhanced Raman scattering from copper phthalocyanine on Pt by use of a Weierstrass prism. *Applied Surface Science* **1996,** *100*, 60-63.

5. Huo, S.-X.; Liu, Q.; Cao, S.-H.; Cai, W.-P.; Meng, L.-Y.; Xie, K.-X.; Zhai, Y.-Y.; Zong, C.; Yang, Z.-L.; Ren, B.; Li, Y.-Q., Surface Plasmon-Coupled Directional Enhanced Raman Scattering by Means of the Reverse Kretschmann Configuration. *The Journal of Physical Chemistry Letters* **2015,** *6* (11), 2015-2019.

6. Futamata, M., Surface Plasmon Polariton Enhanced Raman Scattering from Adsorbates on a "Smooth" Metal Surface: The Effect of Thickness and Dielectric Properties of Constituents. *Langmuir* **1995,** *11* (10), 3894-3901.

7. Byahut, S.; Furtak, T. E., A device for performing surface-plasmon-polariton-assisted Raman scattering from adsorbates on single-crystal silver surfaces. *Review of Scientific Instruments* **1990,** *61* (1), 27-32.

8. Li, H.; Xu, S.; Liu, Y.; Gu, Y.; Xu, W., Directional emission of surface-enhanced Raman scattering based on a planar-film plasmonic antenna. *Thin Solid Films* **2012,** *520* (18), 6001-6006.

9. Wan, X.-m.; Gao, R.; Lu, D.-f.; Qi, Z.-m., Self-referenced directional enhanced Raman scattering using plasmon waveguide resonance for surface and bulk sensing. *Applied Physics Letters* **2018,** *112* (4), 041906.

10. Meyer, S. A.; Le Ru, E. C.; Etchegoin, P. G., Combining Surface Plasmon Resonance (SPR) Spectroscopy with Surface-Enhanced Raman Scattering (SERS). *Analytical Chemistry* **2011,** *83* (6), 2337-2344.

11. Wang, H.; Li, H.; Xu, S.; Zhao, B.; Xu, W., Integrated plasmon-enhanced Raman scattering (iPERS) spectroscopy. *Scientific Reports* **2017,** *7* (1), 14630.

12. Salamon, Z.; Tollin, G., Optical Anisotropy in Lipid Bilayer Membranes: Coupled Plasmon-Waveguide Resonance Measurements of Molecular Orientation, Polarizability, and Shape. *Biophysical Journal* **2001,** *80* (3), 1557-1567.

13. Tollin, G.; Salamon, Z.; Hruby, V. J., Techniques: Plasmon-waveguide resonance (PWR) spectroscopy as a tool to study ligand–GPCR interactions. *Trends in Pharmacological Sciences* **2003,** *24* (12), 655-659.

14. Salamon, Z.; Macleod, H. A.; Tollin, G., Coupled plasmon-waveguide resonators: a new spectroscopic tool for probing proteolipid film structure and properties. *Biophysical Journal* **1997,** *73* (5), 2791-2797.

15. Braundmeier, A. J.; Tomaschke, H. E., Observation of the simultaneous emission of roughness-coupled and optical-coupled surface plasmon radiation from silver. *Optics Communications* **1975,** *14* (1), 99-103.

16. Simon, H. J.; Guha, J. K., Directional surface plasmon scattering from silver films. *Optics Communications* **1976,** *18* (3), 391-394.

17. Meyer, M. W.; McKee, K. J.; Nguyen, V. H. T.; Smith, E. A., Scanning Angle Plasmon Waveguide Resonance Raman Spectroscopy for the Analysis of Thin Polystyrene Films. *The Journal of Physical Chemistry C* **2012,** *116* (47), 24987-24992.

18. McKee, K. J.; Meyer, M. W.; Smith, E. A., Plasmon Waveguide Resonance Raman Spectroscopy. *Analytical Chemistry* **2012,** *84* (21), 9049-9055.

19. M., B. J.; A., S. E., Extracting interface locations in multilayer polymer waveguide films using scanning angle Raman spectroscopy. *Journal of Raman Spectroscopy* **2018,** *49* (2), 262-270.

20. Salamon, Z.; Brown, M. F.; Tollin, G., Plasmon resonance spectroscopy: probing molecular interactions within membranes. *Trends in Biochemical Sciences* **1999,** *24* (6), 213-219.

21. Salamon, Z.; Tollin, G., Plasmon resonance spectroscopy: probing molecular interactions at surfaces and interfaces. *Spectroscopy* **2001,** *15* (3,4).

22. Gryczynski, I.; Malicka, J.; Gryczynski, Z.; Lakowicz, J. R., Radiative decay engineering 4. Experimental studies of surface plasmon-coupled directional emission. *Analytical biochemistry* **2004,** *324* (2), 170-182.

23. Gryczynski, I.; Malicka, J.; Gryczynski, Z.; Nowaczyk, K.; Lakowicz, J. R., Surface plasmon-coupled directional fluorescence emission. *Proceedings of SPIE--the International Society for Optical Engineering* **2004,** *5327* (37), 37-44.

24. Lakowicz, J. R., Radiative decay engineering 3. Surface plasmon-coupled directional emission. *Analytical Biochemistry* **2004,** *324* (2), 153-169.

25. Gryczynski, I.; Malicka, J.; Nowaczyk, K.; Gryczynski, Z.; Lakowicz, J. R., Effects of Sample Thickness on the Optical Properties of Surface Plasmon-Coupled Emission. *The Journal of Physical Chemistry B* **2004,** *108* (32), 12073-12083.

26. Gryczynski, I.; Malicka, J.; Nowaczyk, K.; Gryczynski, Z.; Lakowicz, J. R., Waveguide-modulated surface plasmon-coupled emission of Nile blue in poly(vinyl alcohol) thin films. *Thin Solid Films* **2006,** *510* (1–2), 15-20.

27. Calander, N., Surface Plasmon-Coupled Emission and Fabry−Perot Resonance in the Sample Layer: A Theoretical Approach. *The Journal of Physical Chemistry B* **2005,** *109* (29), 13957-13963.

28. Chen, C.; Li, J.-Y.; Wang, L.; Lu, D.-F.; Qi, Z.-M., Waveguide-coupled directional Raman radiation for surface analysis. *Physical Chemistry Chemical Physics* **2015,** *17* (33), 21278-21287.

29. Chen, C.; Lu, D.-F.; Gao, R.; Qi, Z.-M., Analysis of waveguide-coupled directional emission for efficient collection of Fluorescence/Raman light from surface. *Optics Communications* **2016,** *367*, 86-94.

30. Lakowicz, J. R.; Malicka, J.; Gryczynski, I.; Gryczynski, Z., Directional surface plasmon-coupled emission: a new method for high sensitivity detection. *Biochemical and Biophysical Research Communications* **2003,** *307* (3), 435-439.

31. Malicka, J.; Gryczynski, I.; Gryczynski, Z.; Lakowicz, J. R., DNA Hybridization Using Surface Plasmon-Coupled Emission. *Analytical Chemistry* **2003,** *75* (23), 6629-6633.

32. Calander, N., Theory and Simulation of Surface Plasmon-Coupled Directional Emission from Fluorophores at Planar Structures. *Analytical Chemistry* **2004,** *76* (8), 2168-2173.

33. Abbas, A.; Linman, M. J.; Cheng, Q., Sensitivity comparison of surface plasmon resonance and plasmon-waveguide resonance biosensors. *Sensors and Actuators B: Chemical* **2011,** *156* (1), 169-175.

Table of Contents Figure

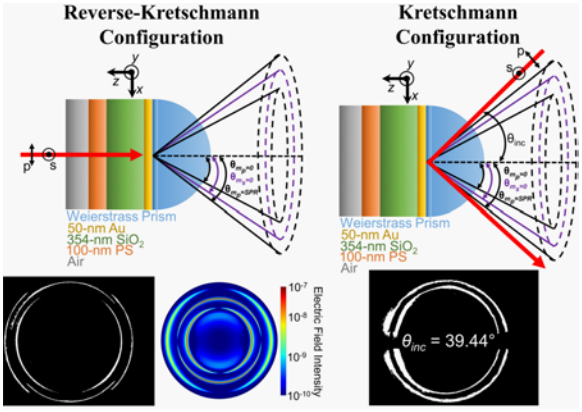

Measured waveguide-coupled surface-plasmon-polariton cone properties with multimodal signal collection represent an alternative method for collecting plasmon waveguide resonance without the need to scan the incident angle or wavelength of light.